한국복합신소재구조학회 논문집 제3권, 제2호, 2012년 6월
J. Korean Soc. Adv. Comp. Struc. Vol. 3, No. 2, pp. 1-10, June 2012
ISSN 2093-5145

활절로 지지된 원통형 적층복합쉘의 기하학적 비선형 해석

한성천[1]

대원대학교 철도건설과 교수[1]

Geometrically Nonlinear Analysis of Hinged Cylindrical Laminated Composite Shells

Han, Sung-Cheon[1]

[1]Department of Civil and Railroad Engineering, Daewon University College

Abstract: In the present study, an Element-Based Lagrangian Formulation for the nonlinear analysis of shell structures is presented. The strains, stresses and constitutive equations based on the natural co-ordinate have been used throughout the Element-Based Lagrangian Formulation of the present shell element which offers an advantage of easy implementation compared with the traditional Lagrangian Formulation. The Element-Based Lagrangian Formulation of a 9-node resultant-stress shell element is presented for the anisotropic composite material. The element is free of both membrane and shear locking behavior by using the assumed natural strain method such that the element performs very well in thin shell problems. The arc-length control method is used to trace complex equilibrium paths in thin shell applications. Numerical examples for laminated composite curved shells presented herein clearly show the validity of the present approach and the accuracy of the developed shell element.

Key Words: 9-node resultant shell element, Element-based Lagrangian Formulation, laminated composite shells, assumed strain method, arc-length control method

1. Introduction

Composite structures offer an attractive alternative to more conventional forms of construction due to its high strength to weight ratio and resistance to corrosion. Recently, there has been a major emphasis made on the use of FRP composite materials as a means of developing new high performance alternative materials for infrastructure applications such as seismic column wrapping and lightweight deck development.

The modeling of shell structures represents a challenging task since the early developments of the finite element method. In fact, papers on the subject (focusing on computational aspects) can be traced back to the original work of Ahmad et al. (1970). This work represented the onset of the so-called degenerated approach, with a three-dimensional continuum being modeled by means of a reference surface. Following this concept, isoparametric finite elements were formulated using independent rotational and displacements degrees of freedom. Further, normal stresses in the direction of the shell thickness were not included in the formulation. The original concept was then extended to the non-linear range in the works of Hughes and Liu (1981) and Liu et al. (1986), among many others.

In large deformation analysis, the linearized non-linear equation has to be derived in order to solve the non-linear equations of the structural system via Lagrangian formulations. Kanok-Nukulchai and Wong (1988) introduced a new

주요어: 9절점 쉘요소, 요소기저 라그랑지안 정식, 적층복합쉘, 자연변형률법, 호장길이법

Corresponding author: Han, Sung-Cheon
Department of Civil and Railroad Engineering, Daewon University College, 599 Shinwol, Jecheon, 390-702, Korea.
Tel: +82-43-649-3267, Fax: +82-43-649-3267, E-mail: hasc1203@daum.net

투고일: 2012년 3월 27일 / 수정일: 2012년 3월 28일 / 게재확정일: 2012년 5월 25일

Lagrangian formulation referred to as the Element-Based Lagrangian Formulation (ELF) since the parental element serves as a deformation reference in ELF. It means that all equations governing a deformed body can be expressed with respect to natural coordinate systems and so it appears in a simpler form than those of the traditional Lagrangian approaches. Lee and Kanok-Nukulchai (1998) presented a 9-node shell element using an Element-Based Lagrangian Formulation concept for large deformation analysis of shell structures. The Element-Based Lagrangian Formulation makes implementation simpler and easier than the traditional Lagrangian formulations, especially when the assumed natural strain method is involved. The shell element is based on the resultant-stress theories with the transverse shear deformation. By using the assumed strain methods, the shell element is free of the membrane and shear locking in the thin shell limit. All the results have very good agreement with references.

However, the development of laminated shell elements for large deformation analysis has been less attempted, than those of single layered isotropic shell elements. In order to develop a laminated shell element for large deformation analysis, a very similar development procedure to that of the single layered shell elements is needed. However, the equivalent constitutive equation should be utilized for the computationally efficient composite element. The resultant shell element concept used an equivalent constitutive equation model which obtains the constitutive law of the equivalent medium in terms of the properties of the individual layers. Recently, Han et al. (2004, 2006, 2008(a), 2008(b), 2011) and Park et al. (2010) presented linear and nonlinear analysis of laminated composite plates and shells.

The objective of this paper is to present the formulation of a geometrically nonlinear 9-node shell element based on the resultant-stress formulation and its application to geometrical nonlinear analysis of laminate composite shell structures. The ELF concept is adopted to present the initial configuration and deformed configurations of the present finite element. The assumed natural strain method has been used to remove the locking problems by the ELF form. The formulation of the resultant shell element is based on Mindlin-Reissner theory, assuming small strains and large rotations. The geometric stiffness is analytically integrated through the thickness. In comparison with volume integration, which is generally used in the degenerated shell elements, the computational time is significantly reduced for geometrically nonlinear analysis of laminated composite structures.

2. Geometry and Kinematics of the Shell Element

Generally the Lagrangian formulations for geometric nonlinear case can be classified into two approaches: namely, (1) Total Lagrangian Formulation (TLF), where all the static and kinematic variables are referred back to the initial undeformed configuration (B_o), (2) Updated Lagrangian Formulation (ULF), where all are referred to the current deformed configuration (B_t).

Wong (1984) has proposed a new variation of Lagrangian formulation known as Element-based Lagrangian Formulation (ELF), where all the static and kinematic variables are referred to a nonphysical *"Element-based"* configuration ($\bar{B}$) as shown in Fig. 1. Unlike the two traditional Lagrangian formulations, a standard parental element serving as the reference of deformation is to be mapped directly into each element of the initial and deformed configurations in the Element-based Lagrangian Formulation. Therefore, all balance equations governing the deformed configuration can be expressed over the parental element domain in terms of the element natural co-ordinates. It should be noted that these three approaches for a problem should theoretically yield the same result.

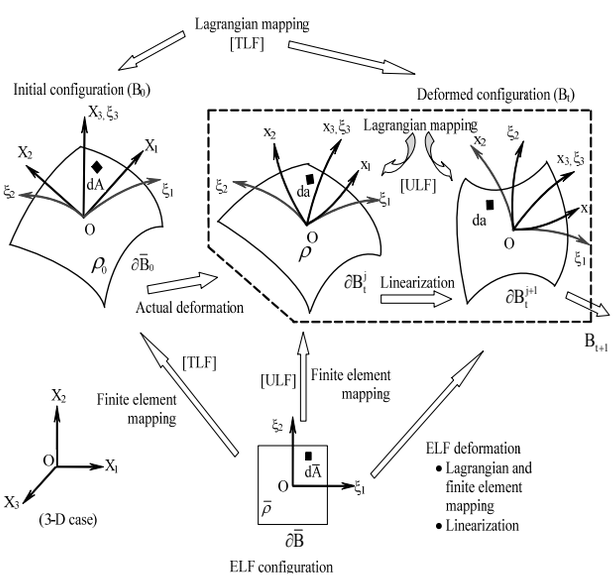

Fig. 1 The Element-Based Lagrangian Formulation method

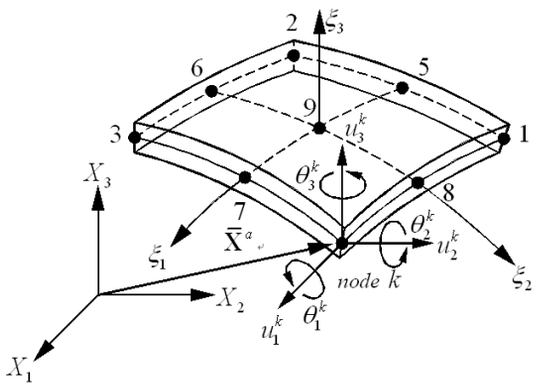

Fig. 2 Geometry of 9-node shell element with six degrees of freedom

The geometry of 9-node shell element shown in Fig. 2 has six degrees of freedom per node. The initial geometry of the nine-node Lagrangian element shown in Fig. 3 is defined by the following relations. The initial configuration of the shell element having constant thickness h can be written as

$$\mathbf{X}(\xi_1,\xi_2,\xi_3) = \bar{\mathbf{X}}(\xi_1,\xi_2) + \mathbf{D}(\xi_1,\xi_2,\xi_3) \tag{1}$$

where

$$\bar{\mathbf{X}}(\xi_1,\xi_2) = \sum_{a=1}^{9} N^a(\xi_1,\xi_2)\bar{\mathbf{X}}^a$$
$$\mathbf{D}(\xi_1,\xi_2,\xi_3) = \sum_{a=1}^{9} N^a(\xi_1,\xi_2)\mathbf{D}^a$$
$$\mathbf{D}^a(\xi_3) = \frac{h^a\xi_3}{2}\hat{\mathbf{D}}^a \tag{2}$$

where $\bar{X}^a$ are position vectors at midsurface which have three Cartesian components, D^a are nine unit normal vectors and $\hat{D}^a$ is a unit normal vector at node a.

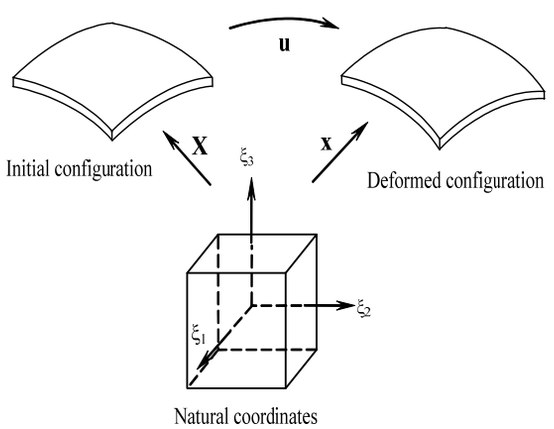

Fig. 3 Initial and deformed geometries of a shell element

The following relations are introduced for the definition of deformed geometry of the element.

$$\mathbf{x}(\xi_1,\xi_2,\xi_3) = \sum_{a=1}^{9} N^a(\xi_1,\xi_2)\left[\bar{\mathbf{x}}^a + \frac{\xi_3 h^a}{2}\hat{\mathbf{d}}^a\right] = \bar{\mathbf{x}} + \xi_3\bar{\mathbf{d}} \tag{3}$$

In Eq. (3), $\mathbf{x},\bar{\mathbf{x}},\bar{\mathbf{d}},\bar{\mathbf{x}}_a,\mathbf{d}^a$ and $\hat{\mathbf{d}}^a$ in the deformed geometry correspond to $\mathbf{X},\bar{\mathbf{X}},\bar{\mathbf{D}},\bar{\mathbf{X}}^a,\mathbf{D}^a$ and $\hat{\mathbf{D}}^a$ in Eqs. (1)-(2). Hence, the displacement field u in the shell element can be defined as

$$\mathbf{u}(\xi_1,\xi_2,\xi_3) = \sum_{a=1}^{9} N^a(\xi_1,\xi_2)\left[\bar{\mathbf{u}}^a + \frac{\xi_3 h^a}{2}\hat{\mathbf{e}}^a\right] = \bar{\mathbf{u}} + \xi_3\bar{\mathbf{e}} \tag{4}$$

where, at the node a the translational displacement vector $\bar{\mathbf{u}}^a = \bar{\mathbf{x}}^a - \bar{\mathbf{X}}^a$, and the fibre displacement vector $\hat{\mathbf{e}}^a = \hat{\mathbf{d}}^a - \hat{\mathbf{D}}^a$.

The translation displacement field can be expressed by shape functions in terms of nodal translational as shown in the first part of the right-hand side of Eq. (4). The three successive rotations θ_1, θ_2 and θ_3 have been introduced to express finite rotational displacement instead of the Euler angle which usually guarantees the independence of two rotations in the Lagrangian formulation since six degrees of freedom are adopted in the present study. If we introduce another set of Cartesian co-ordinates at the nodal points with the assumption that the unit normal vectors are firmly fixed into it and they move with the body, rotations which are undergone by the unit normal vector during deformation could be expressed elegantly via this co-ordinate set.

Basically, the transformation matrices for these rotations are

$$T_{R1}(\theta_1) = \begin{bmatrix} 1 & 0 & 0 \\ 0 & \cos\theta_1 & -\sin\theta_1 \\ 0 & \sin\theta_1 & \cos\theta_1 \end{bmatrix}$$
$$T_{R2}(\theta_2) = \begin{bmatrix} \cos\theta_2 & 0 & \sin\theta_2 \\ 0 & 1 & 0 \\ -\sin\theta_2 & 0 & \cos\theta_2 \end{bmatrix}$$
$$T_{R3}(\theta_3) = \begin{bmatrix} \cos\theta_3 & -\sin\theta_3 & 0 \\ \sin\theta_3 & \cos\theta_3 & 0 \\ 0 & 0 & 1 \end{bmatrix} \tag{5}$$

However, it is important to note that three successive rotations used in this study lost their vectorial characteristics which remained in the cases when the rotations were infinitesimal. After undergoing three rotations successively, the transformation matrix between the initial shell normal and the deformed normal can be written as the result of a sequence of finite rotations θ_1 , θ_2 and θ_3 as follows;

$$\mathbf{T_R} = T_{R1}(\theta_1)T_{R2}(\theta_2)T_{R3}(\theta_3)$$

$$= \begin{bmatrix} \cos\theta_2\cos\theta_3 & -\cos\theta_2\sin\theta_3 & \sin\theta_2 \\ \cos\theta_1\sin\theta_3+\sin\theta_1\sin\theta_2\cos\theta_3 & \cos\theta_1\cos\theta_3-\sin\theta_1\sin\theta_2\sin\theta_3 & -\sin\theta_1\cos\theta_2 \\ \sin\theta_1\sin\theta_3-\cos\theta_1\sin\theta_2\cos\theta_3 & \sin\theta_1\cos\theta_3+\cos\theta_1\sin\theta_2\sin\theta_3 & \cos\theta_1\cos\theta_2 \end{bmatrix} \tag{6}$$

Consequently, using the transformation matrix of Eq. (6), the displacement field in Eq. (4) can be expressed as

$$\mathbf{u}(\xi_1,\xi_2,\xi_3) = \sum_{a=1}^{9} N^a(\xi_1,\xi_2)\left[\bar{\mathbf{u}}^a + \frac{\xi_3 h^a}{2}(\mathbf{T}_\mathbf{R}^a - \mathbf{I}_{3\times3})\hat{\mathbf{D}}^a\right] \tag{7}$$

where $\mathbf{I}_{3\times3}$ is a unit matrix.

In addition, with some mathematical manipulation, the incremental form of the displacement field for the present shell element may be written in terms of the nodal incremental vector $\Delta\mathbf{U}^a$ as

$$\Delta\mathbf{u}(\xi_1,\xi_2,\xi_3) = \sum_{a=1}^{9} N^a(\xi_1,\xi_2)\left[\mathbf{I}_{3\times3}\left|\xi_3\mathbf{V}^a\right.\right]\Delta\mathbf{U}^a \tag{8}$$

where

$$\mathbf{V}^a = \frac{h^a}{2}\mathbf{T}_\mathbf{R}^a\mathbf{\Phi}^a\mathbf{T}_\mathbf{A},$$

$$\Delta\mathbf{U}^a = \left\{\Delta\bar{u}_1^a, \Delta\bar{u}_2^a, \Delta\bar{u}_3^a, \Delta\theta_1^a, \Delta\theta_2^a, \Delta\theta_3^a\right\} \tag{9}$$

in which

$$\mathbf{\Phi}^a = \begin{bmatrix} 0 & \hat{D}_3^a & -\hat{D}_2^a \\ -\hat{D}_3^a & 0 & \hat{D}_1^a \\ \hat{D}_2^a & -\hat{D}_1^a & 0 \end{bmatrix};$$

$$\mathbf{T_A} = \begin{bmatrix} \cos\theta_2\cos\theta_3 & \sin\theta_3 & 0 \\ -\cos\theta_2\sin\theta_3 & \cos\theta_3 & 0 \\ \sin\theta_2 & 0 & 1 \end{bmatrix} \tag{10-1, 2}$$

3. Natural Strain Tensor

In the Element-based Lagrangian formulation, an Element-based strain tensor will be defined with respect to the convected curvilinear coordinates (ξ_1,ξ_2,ξ_3) as

$$\tilde{E}_{\alpha\beta} = \frac{1}{2}\left(g_{\alpha\beta} - G_{\alpha\beta}\right) \tag{11}$$

in which $g_{\alpha\beta}$ and $G_{\alpha\beta}$ are the covariant components of the metric tensors to be obtained from the basis vector $g_\alpha = \frac{\partial x_i}{\partial \xi_\alpha}\mathbf{I}_i$ and $G_\beta = \frac{\partial X_I}{\partial \xi_\beta}\mathbf{I}_I$ which are tangents to the curvilinear coordinate lines in $\mathbf{B}_t$ and $\mathbf{B}_0$ respectively, i.e.,

$$g_{\alpha\beta} = g_\alpha \cdot g_\beta = \frac{\partial x_i}{\partial\xi_\alpha}\frac{\partial x_i}{\partial\xi_\beta},$$

$$G_{\alpha\beta} = G_\alpha \cdot G_\beta = \frac{\partial X_I}{\partial\xi_\alpha}\frac{\partial X_I}{\partial\xi_\beta} \tag{12}$$

Two major different definitions of strain, the so-called Lagrangian strain and the Eulerian strain, which depend on the reference system measuring the deformation, have been extensively used in the formulation of large deformation analysis. However, since the formulation used in this study refers to the natural reference system, following the element-based Lagrangian formulation (Kanok-Nukulchai and Wong, 1988), the natural strain tensor corresponding to the Green strain tensor may be defined as

$$\tilde{E}_{\alpha\beta} = \frac{1}{2}\left(\frac{\partial x_i}{\partial\xi_\alpha}\frac{\partial x_i}{\partial\xi_\beta} - \frac{\partial X_I}{\partial\xi_\alpha}\frac{\partial X_I}{\partial\xi_\beta}\right) \tag{13}$$

It should be noted that the Green strain tensor and the natural strain have the following tensor transformation relationship.

$$\tilde{E}_{\alpha\beta} = \frac{\partial X_I}{\partial\xi_\alpha}\frac{\partial X_J}{\partial\xi_\beta}E_{IJ}$$

$$= \frac{1}{2}\left[\frac{\partial X_I}{\partial\xi_\alpha}\frac{\partial u_I}{\partial\xi_\beta} + \frac{\partial u_J}{\partial\xi_\alpha}\frac{\partial X_J}{\partial\xi_\beta} + \frac{\partial u_K}{\partial\xi_\alpha}\frac{\partial u_K}{\partial\xi_\beta}\right] \tag{14}$$

By substituting Eq. (1) and Eq. (4) in Eq. (14), and using a shifter transformation between the local and global displacement, the following strain-displacement relation can be obtained

$$\tilde{E}_{\alpha\beta}=\frac{1}{2}\left[\frac{\partial\left(\bar{X}_I+\xi_3\bar{D}_I\right)}{\partial\xi_\alpha}\frac{\partial\left(\bar{u}_I+\xi_3\bar{e}_I\right)}{\partial\xi_\beta}+\frac{\partial\left(\bar{u}_J+\xi_3\bar{e}_J\right)}{\partial\xi_\alpha}\frac{\partial\left(\bar{X}_J+\xi_3\bar{D}_J\right)}{\partial\xi_\beta}\right.$$
$$\left.+\frac{\partial\left(\bar{u}_K+\xi_3\bar{e}_K\right)}{\partial\xi_\alpha}\frac{\partial\left(\bar{u}_K+\xi_3\bar{e}_K\right)}{\partial\xi_\beta}\right] \quad (15)$$

The incremental membrane, bending and transverse shear strains with Eq. (9) can be separated into linear and nonlinear parts such as:

$$\Delta\tilde{E}^m=\Delta^L\tilde{E}^m+\Delta^{NL}\tilde{E}^m$$
$$\Delta\tilde{E}^b=\Delta^L\tilde{E}^b+\Delta^{NL}\tilde{E}^b$$
$$\Delta\tilde{E}^s=\Delta^L\tilde{E}^s+\Delta^{NL}\tilde{E}^s \quad (16)$$

where

$$\Delta^L\tilde{E}^m=\begin{bmatrix}\frac{\partial\bar{X}_1}{\partial\xi_1}\frac{\partial}{\partial\xi_1} & 0 & 0\\ 0 & \frac{\partial\bar{X}_2}{\partial\xi_2}\frac{\partial}{\partial\xi_2} & 0\\ \frac{1}{2}\left(\frac{\partial\bar{X}_1}{\partial\xi_1}\frac{\partial}{\partial\xi_2}\right) & \frac{1}{2}\left(\frac{\partial\bar{X}_2}{\partial\xi_2}\frac{\partial}{\partial\xi_1}\right) & 0\end{bmatrix}\begin{Bmatrix}\Delta\bar{u}_1\\ \Delta\bar{u}_2\\ \Delta\bar{u}_3\end{Bmatrix}=\tilde{\mathbf{B}}_{\mathbf{m}}\Delta\mathbf{U} \quad (17)$$

$$\Delta^L\tilde{E}^b=\xi_3\begin{bmatrix}\frac{\partial\bar{D}_1}{\partial\xi_1}\frac{\partial}{\partial\xi_1} & 0 & 0\\ 0 & \frac{\partial\bar{D}_2}{\partial\xi_2}\frac{\partial}{\partial\xi_2} & 0\\ \frac{1}{2}\left(\frac{\partial\bar{D}_1}{\partial\xi_1}\frac{\partial}{\partial\xi_2}\right) & \frac{1}{2}\left(\frac{\partial\bar{D}_2}{\partial\xi_2}\frac{\partial}{\partial\xi_1}\right) & 0\end{bmatrix}\begin{bmatrix}\frac{\partial\bar{X}_1}{\partial\xi_1}\frac{\partial}{\partial\xi_1} & 0 & 0\\ 0 & \frac{\partial\bar{X}_2}{\partial\xi_2}\frac{\partial}{\partial\xi_2} & 0\\ \frac{1}{2}\left(\frac{\partial\bar{X}_1}{\partial\xi_1}\frac{\partial}{\partial\xi_2}\right) & \frac{1}{2}\left(\frac{\partial\bar{X}_2}{\partial\xi_2}\frac{\partial}{\partial\xi_1}\right) & 0\end{bmatrix}\begin{Bmatrix}\Delta\bar{u}_1\\ \Delta\bar{u}_2\\ \Delta\bar{u}_3\\ \Delta\bar{e}_1\\ \Delta\bar{e}_2\\ \Delta\bar{e}_3\end{Bmatrix}=\xi_3\tilde{\mathbf{B}}_{\mathbf{b}}\Delta\mathbf{U} \quad (18)$$

$$\Delta^L\tilde{E}^s=\begin{bmatrix}0 & 0 & \frac{1}{2}\left(\bar{D}_3\frac{\partial}{\partial\xi_2}\right) & 0 & \frac{1}{2}\frac{\partial\bar{X}_2}{\partial\xi_2} & 0\\ 0 & 0 & \frac{1}{2}\left(\bar{D}_3\frac{\partial}{\partial\xi_1}\right) & \frac{1}{2}\frac{\partial\bar{X}_1}{\partial\xi_1} & 0 & 0\end{bmatrix}\begin{Bmatrix}\Delta\bar{u}_1\\ \Delta\bar{u}_2\\ \Delta\bar{u}_3\\ \Delta\bar{e}_1\\ \Delta\bar{e}_2\\ \Delta\bar{e}_3\end{Bmatrix}=\tilde{\mathbf{B}}_{\mathbf{s}}\Delta\mathbf{U} \quad (19)$$

In Eq. (18), $\tilde{\mathbf{B}}_{\mathbf{b}}$ is the bending strain matrix which cooperates the coupling term between the bending strain and displacement, which is different from the formulation by Lee and Kanok-Nukulchai (1998). The additional terms in the two first columns of $\tilde{\mathbf{B}}_{\mathrm{b}}$ reflect the contributions of warping problem shown in the numerical examples 1.

The present strain-displacement $\tilde{\mathbf{B}}$ matrix may be derived from the assumed displacement field using the above definition.

$$\begin{Bmatrix}\Delta^L\tilde{E}_m\\ \Delta^L\tilde{E}_b\\ \Delta^L\tilde{E}_s\end{Bmatrix}_{8\times1}=\begin{bmatrix}\tilde{\mathbf{B}}_{\mathbf{m}} & 0\\ \xi_3\tilde{\mathbf{B}}_{\mathbf{b1}} & \xi_3\tilde{\mathbf{B}}_{\mathbf{b2}}\\ \tilde{\mathbf{B}}_{\mathbf{s1}} & \tilde{\mathbf{B}}_{\mathbf{s2}}\end{bmatrix}_{8\times6}\begin{Bmatrix}\Delta\mathbf{u}\\ \Delta\boldsymbol{\theta}\end{Bmatrix}_{6\times1} \quad (20)$$

In order to remove the locking behaviour, the assumed natural strains described in the following section have been derived and a new $\tilde{\mathbf{B}}_{\mathrm{AS}}$ matrix has been implemented instead of using the standard $\tilde{\mathbf{B}}$ matrix.

4. Transverse Shear and Membrane Locking

In order to avoid locking problems, the assumed natural strain method in the 8-node shell element by Kim et al. (2003) is used to the 9-node composite shell element. Thus the transverse shear and membrane strain fields are interpolated with the following sampling points in Fig 4.

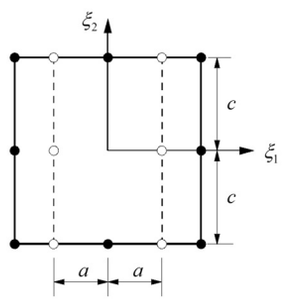

(a) Membrane normal strain

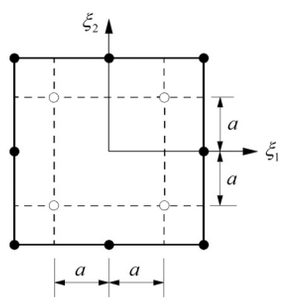

(b) Membrane shear strain

Fig. 4 Sampling points for assumed strains of $\tilde{e}_{11}, \tilde{e}_{13}$, $\tilde{e}_{22}, \tilde{e}_{23}$ **and** $\tilde{e}_{12}$ (a : $\sqrt{1/3}$, c : 1.0)

The interpolation function for assumed natural strain is shown in the following Table 1.

For assumed membrane strains $\tilde{e}_{11}, \tilde{e}_{22}$ and assumed transverse shear strain $\tilde{e}_{13}, \tilde{e}_{23}$ the following sampling points are used as shown in Figure 4:

$$\begin{aligned}
&\tilde{e}_{13}, \tilde{e}_{11} \;>> \\
&(1/\sqrt{3}, 1)_1 : (1/\sqrt{3}, 0)_2 : (1/\sqrt{3}, -1)_3 : \\
&(-1/\sqrt{3}, 1)_4 : (-1/\sqrt{3}, 0)_5 : (-1/\sqrt{3}, -1)_6 \\
&\tilde{e}_{23}, \tilde{e}_{22} \;>> \\
&(1, 1/\sqrt{3})_1 : (0, 1/\sqrt{3})_2 : (-1, 1/\sqrt{3})_3 : \\
&(1, -1/\sqrt{3})_4 : (0, -1/\sqrt{3})_5 : (-1, -1/\sqrt{3})_6
\end{aligned} \tag{21}$$

On the other hand, the standard 2 x 2

Gauss-Legendre numerical integration points are used as sampling points of the assumed membrane shear strain $\tilde{e}_{12}$. Using these three kinds of sampling points, we can establish assumed strains as

$$\tilde{e}_{13} = \tilde{H}^1 \tilde{E}_{13}^{\delta 1} \;,\; \tilde{e}_{23} = \tilde{H}^2 \tilde{E}_{23}^{\delta 1} \;,\; \tilde{e}_{12} = \tilde{H}^3 \tilde{E}_{12}^{\delta 2} \quad \text{k} \tag{22}$$

in which $\tilde{E}_{13}^{\delta 1}$, $\tilde{E}_{23}^{\delta 1}$, $\tilde{E}_{12}^{\delta 2}$ refer to the strains at the sampling points, $\delta 1 = 3(i-1) + j$ denotes the position of the sampling point for $\tilde{e}_{11}, \tilde{e}_{22}, \tilde{e}_{13}, \tilde{e}_{23}$ and $\delta 2 = 2(i-1) + j$ denotes the position of the sampling point for $\tilde{e}_{12}$ as shown in Figure 4.

The remaining terms of Eq. (21), the assumed strain $\tilde{e}_{11}, \tilde{e}_{22}$, have the same interpolation scheme as $\tilde{e}_{13}, \tilde{e}_{23}$, respectively.

The incremental assumed natural membrane strains with Eq. (22) can be written as

$$\begin{aligned}
\Delta^L \tilde{e}_{11}^m &= \tilde{H}^1 \left\{ \left[\frac{\partial \bar{X}_1}{\partial \xi_1} \frac{\partial}{\partial \xi_1} \right] \{ \Delta \bar{u}_1 \} \right\}^{\delta 1}, \\
\Delta^L \tilde{e}_{22}^m &= \tilde{H}^2 \left\{ \left[\frac{\partial \bar{X}_2}{\partial \xi_2} \frac{\partial}{\partial \xi_2} \right] \{ \Delta \bar{u}_2 \} \right\}^{\delta 1}, \\
\Delta^L \tilde{e}_{12}^m &= \tilde{H}^2 \left\{ \left[\frac{1}{2} \frac{\partial \bar{X}_1}{\partial \xi_1} \frac{\partial}{\partial \xi_2} \quad \frac{1}{2} \frac{\partial \bar{X}_2}{\partial \xi_2} \frac{\partial}{\partial \xi_1} \right] \begin{Bmatrix} \Delta \bar{u}_1 \\ \Delta \bar{u}_2 \end{Bmatrix} \right\}^{\delta 2}
\end{aligned} \tag{23}$$

Eq. (23) can be expressed as following form

$$\Delta^L \tilde{e}^m = \left(\tilde{\mathbf{B}}_{\mathbf{m}} \right)_{AS} \Delta \bar{\mathbf{u}} \tag{24}$$

The incremental assumed natural transverse shear strains with Eq. (22) can be written as

$$\begin{aligned}
\Delta^L \tilde{e}_{13}^s &= \tilde{H}^1 \left\{ \begin{bmatrix} \frac{1}{2} \bar{D}_3 \frac{\partial}{\partial \xi_1} & \frac{1}{2} \frac{\partial \bar{X}_1}{\partial \xi_1} \end{bmatrix} \begin{Bmatrix} \Delta \bar{u}_3 \\ \Delta \bar{e}_1 \end{Bmatrix} \right\}^{\delta 1}, \\
\Delta^L \tilde{e}_{23}^s &= \tilde{H}^2 \left\{ \begin{bmatrix} \frac{1}{2} \bar{D}_3 \frac{\partial}{\partial \xi_2} & \frac{1}{2} \frac{\partial \bar{X}_2}{\partial \xi_2} \end{bmatrix} \begin{Bmatrix} \Delta \bar{u}_3 \\ \Delta \bar{e}_2 \end{Bmatrix} \right\}^{\delta 1}
\end{aligned} \tag{25}$$

Eq. (25) can be expressed as following form

$$\Delta^L \tilde{e}^s = \left[\left(\tilde{\mathbf{B}}_{s1} \right)_{AS} \quad \left(\tilde{\mathbf{B}}_{s2} \right)_{AS} \right] \begin{Bmatrix} \Delta \bar{\mathbf{u}} \\ \Delta \boldsymbol{\theta} \end{Bmatrix} = \left(\tilde{\mathbf{B}}_{\mathbf{s}} \right)_{AS} \Delta \mathbf{U} \tag{26}$$

Eq. (24) and Eq. (26) can be expressed in the following form:

$$\begin{Bmatrix} \Delta^L \tilde{e}^m \\ \Delta^L \tilde{E}^b \\ \Delta^L \tilde{e}^s \end{Bmatrix}_{8\times 1} = \begin{bmatrix} \left(\tilde{\mathbf{B}}_{\mathbf{m}} \right)_{AS} & 0 \\ \xi_3 \tilde{\mathbf{B}}_{\mathbf{b1}} & \xi_3 \tilde{\mathbf{B}}_{\mathbf{b2}} \\ \left(\tilde{\mathbf{B}}_{\mathbf{s1}} \right)_{AS} & \left(\tilde{\mathbf{B}}_{\mathbf{s2}} \right)_{AS} \end{bmatrix}_{8\times 6} \begin{Bmatrix} \Delta \bar{\mathbf{u}} \\ \Delta \boldsymbol{\theta} \end{Bmatrix}_{6\times 1} \tag{27}$$

Table 1. Interpolation function for assumed natural strain fields

i	$\tilde{H}^i$	$*P_i(\xi_1)$	$*Q_i(\xi_2)$
1	$\sum_{i=1}^{2}\sum_{j=1}^{3} P_i(\xi_1) Q_j(\xi_2)$	$P_1(\xi_1) = \frac{1}{2}\left(1+\sqrt{3}\xi_1\right)$	$Q_1(\xi_2) = \frac{1}{2}\xi_2(\xi_2+1)$
2	$\sum_{i=1}^{2}\sum_{j=1}^{3} P_i(\xi_2) Q_j(\xi_1)$	$P_2(\xi_1) = \frac{1}{2}\left(1-\sqrt{3}\xi_1\right)$	$Q_2(\xi_2) = 1-\xi_2^2$
3	$\sum_{i=1}^{2}\sum_{j=1}^{2} P_i(\xi_1) P_j(\xi_2)$	-	$Q_3(\xi_2) = \frac{1}{2}\xi_2(\xi_2-1)$

* $P(\xi_2)$ and $Q(\xi_1)$ can be obtained by changing variables.

5. Constitutive Equation

In order to obtain a natural co-ordinate based constitutive equation, we introduce here an explicit transformation scheme between natural co-ordinates and the global co-ordinate system.

$$\mathbf{S} = \tilde{J}_0 \mathbf{T}\,\mathbf{D}\,\mathbf{T}^{\mathrm{T}}\tilde{\mathbf{E}} = \tilde{\mathbf{C}}\,\tilde{\mathbf{E}} \tag{28}$$

where $\tilde{J}_0$ is the determinant of the Jacobian matrix, $\mathbf{D}$ is the constitutive matrix for orthotropic materials with the material angle θ is given by

$$\mathbf{D} = \mathbf{T}_1 \mathbf{C}\,\mathbf{T}_1^{\mathrm{T}} \tag{29}$$

where $\mathbf{C}$ is the constitutive matrix for orthotropic materials and $\mathbf{T}_1$ is the transformation matrix between local and material axis.

The transformation matrix $\mathbf{T}$ in Eq. (28) is given as

$$\mathbf{T} = \begin{bmatrix} \chi_{11}\chi_{11} & \chi_{21}\chi_{21} & \chi_{31}\chi_{31} & 2\chi_{11}\chi_{21} & 2\chi_{21}\chi_{31} & 2\chi_{11}\chi_{31} \\ \chi_{12}\chi_{12} & \chi_{22}\chi_{22} & \chi_{32}\chi_{32} & 2\chi_{12}\chi_{22} & 2\chi_{22}\chi_{32} & 2\chi_{12}\chi_{32} \\ \chi_{13}\chi_{13} & \chi_{23}\chi_{23} & \chi_{33}\chi_{33} & 2\chi_{13}\chi_{23} & 2\chi_{23}\chi_{33} & 2\chi_{13}\chi_{33} \\ \chi_{11}\chi_{12} & \chi_{21}\chi_{22} & \chi_{31}\chi_{32} & \chi_{11}\chi_{22}+\chi_{12}\chi_{21} & \chi_{21}\chi_{32}+\chi_{22}\chi_{31} & \chi_{11}\chi_{32}+\chi_{12}\chi_{31} \\ \chi_{12}\chi_{13} & \chi_{22}\chi_{23} & \chi_{32}\chi_{33} & \chi_{12}\chi_{23}+\chi_{13}\chi_{22} & \chi_{22}\chi_{33}+\chi_{23}\chi_{32} & \chi_{12}\chi_{33}+\chi_{13}\chi_{32} \\ \chi_{11}\chi_{13} & \chi_{21}\chi_{23} & \chi_{31}\chi_{33} & \chi_{11}\chi_{23}+\chi_{13}\chi_{21} & \chi_{21}\chi_{33}+\chi_{23}\chi_{31} & \chi_{11}\chi_{33}+\chi_{13}\chi_{31} \end{bmatrix} \tag{30}$$

where

$$\chi_{ij} = \frac{\partial \xi_j}{\partial X_i} \tag{31}$$

The shell element displays resultant membrane forces ($\mathbf{N}$), moments($\mathbf{M}$) and transverse shear forces($\mathbf{Q}$) acting on a laminate which are obtained by integration of stresses through the laminate thickness. In this study, we impose the plane state on the natural constitutive equation of Eq. (28) before forming the equivalent constitutive equation. The compact incremental constitutive relations of the composite laminate are as follows:

$$\begin{Bmatrix} \Delta\mathbf{N} \\ \Delta\mathbf{M} \\ \Delta\mathbf{Q} \end{Bmatrix} = \begin{bmatrix} [\mathbf{A}] & [\mathbf{B}] & \mathbf{0} \\ [\mathbf{B}] & [\mathbf{D}] & \mathbf{0} \\ \mathbf{0} & \mathbf{0} & [\mathbf{G}] \end{bmatrix} \begin{Bmatrix} \Delta^{L}\tilde{E}^{m} \\ \Delta^{L}\tilde{E}^{b} \\ \Delta^{L}\tilde{E}^{s} \end{Bmatrix} \tag{32}$$

where

$$\begin{aligned}
[\mathbf{A}]_{3\times3} &= \int \tilde{\mathbf{C}}_{\mathbf{mb}} d\xi_3 = \sum_{k=1}^{N}\int_{t_{k-1}}^{t_k} \tilde{\mathbf{C}}_{\mathbf{mb}} d\xi_3 = \sum_{k=1}^{N} \tilde{\mathbf{C}}_{\mathbf{mb}}^{k}\left(\xi_3^{k} - \xi_3^{k-1}\right), \\
[\mathbf{B}]_{3\times3} &= \int \xi_3 \tilde{\mathbf{C}}_{\mathbf{mb}} d\xi_3 = \sum_{k=1}^{N}\int_{t_{k-1}}^{t_k} \xi_3 \tilde{\mathbf{C}}_{\mathbf{mb}} d\xi_3 = \frac{1}{2}\sum_{k=1}^{N} \tilde{\mathbf{C}}_{\mathbf{mb}}^{k}\left(\left(\xi_3^{k}\right)^2 - \left(\xi_3^{k-1}\right)^2\right), \\
[\mathbf{D}]_{3\times3} &= \int \xi_3^{\,2} \tilde{\mathbf{C}}_{\mathbf{mb}} d\xi_3 = \sum_{k=1}^{N}\int_{t_{k-1}}^{t_k} \xi_3^{\,2} \tilde{\mathbf{C}}_{\mathbf{mb}} d\xi_3 = \frac{1}{3}\sum_{k=1}^{N} \tilde{\mathbf{C}}_{\mathbf{mb}}^{k}\left(\left(\xi_3^{k}\right)^3 - \left(\xi_3^{k-1}\right)^3\right), \\
[\mathbf{G}]_{2\times2} &= \int k_s \tilde{\mathbf{C}}_{\mathbf{s}} d\xi_3 = k_s \sum_{k=1}^{N}\int_{t_{k-1}}^{t_k} \tilde{\mathbf{C}}_{\mathbf{s}} d\xi_3 = k_s \sum_{k=1}^{N} \tilde{\mathbf{C}}_{\mathbf{s}}^{k}\left(\xi_3^{k} - \xi_3^{k-1}\right)
\end{aligned} \tag{33}$$

Here k is the layer number, N is the total number of layers of the shell, $\tilde{\mathbf{C}}_{\mathbf{mb}} = \tilde{\mathbf{C}}_{ij}\,(i,j=1,2,3)$, $\tilde{\mathbf{C}}_{\mathbf{s}} = \tilde{\mathbf{C}}_{ij}\,(i,j=4,5)$ and k_s is the transverse shear correction factor. Reissner's value of 5/6 is used as the transverse shear correction factor in the finite element formulation.

6. Incremental Equation of Equilibrium

The generalized Hook's law at large strain does not represent an approximate material behavior description because stress-strain relation is non-linear. From the practical point of view, Hook's law is only applicable to small strain, which constitutive tensor is constant coefficient. Using small strain assumption, the following incremental equilibrium equation is obtained.

$$\int \delta\left(\Delta^{L}\tilde{E}\right)^{T} \tilde{\mathbf{C}} \Delta^{L}\tilde{E}\, dV + \int \mathbf{S}\left(\Delta^{NL}\tilde{E}\right) dV = {}^{t+\Delta t}\delta W_{ext} - \int \delta\left(\Delta^{L}\tilde{E}\right)^{T} \mathbf{S}\, dV \tag{34}$$

where $\tilde{\mathbf{C}}$ is the constitutive matrix for orthotropic materials with the material angle θ, superscript t which is generally used as the current configuration is ignored in the above Eq. (34) and superscript $t+\Delta t$ is the adjust incremented configuration, ${}^{t+\Delta t}\delta W_{ext}$ is the external virtual work in $t+\Delta t$.

The total tangent stiffness comprises the material stiffness and the geometric stiffness. The linear part of the Green strain tensor is used to derive the material stiffness matrix and non-linear part of the Green strain tensor is used to derive the geometric stiffness matrix.

6.1 Linear Element Stiffness Matrix

If the strain-displacement Eq. (16) is substituted into Eq. (34), the linear element material stiffness matrix ($[\mathbf{K}_L]$) is obtained.

$$\int \delta(\Delta^L\tilde{E})^T \tilde{\mathbf{C}}\, \Delta^L\tilde{E}\, dV = \delta\Delta\mathbf{u}^T \left(\int \tilde{\mathbf{B}}^T \tilde{\mathbf{C}}\, \tilde{\mathbf{B}}\, dV\right)\Delta\mathbf{u} = \delta\Delta\mathbf{u}^T [\mathbf{K}_L]\Delta\mathbf{u} \tag{35}$$

The element stiffness matrix may be written in a matrix form using the equivalent constitutive equations. Finally the element stiffness matrix has 6x6 size on the reference-surface of shell element. The torsional stiffness term was formed as described in Kanok- Nukulchai (1988) and added to the stiffness term.

6.2 Geometric Stiffness Matrix

In order to obtain an accurate geometric stiffness matrix, the stresses should be evaluated accurately. The accuracy of the computation of stresses for formulation of geometric stiffness matrix is maintained by obtaining the same interpolated strains in the computation of linear stiffness matrix. The stresses are computed at the integration points based on these strains. Substituting the non-linear part of strain into Eq. (35), the following geometric stiffness matrix($[\mathbf{K}_G]$) is obtained.

$$\int \delta\left(\Delta^{NL}\tilde{E}\right)^T \tilde{\mathbf{C}}\, \Delta^{NL}\tilde{E}\, dV + \int \mathbf{S}\left(\Delta^{NL}\tilde{E}\right) dV = \delta\Delta\mathbf{u}^T [\mathbf{K}_G]\Delta\mathbf{u} \tag{36}$$

The geometric stiffness matrix in the natural coordinate is analytically integrated through the thickness. By the transformation the natural to the global frame, the element geometric stiffness matrix is obtained on the global frame with 6x6 sub-matrix.

Then the final assembled incremental non-linear equilibrium equation can be written is

$$\left([\mathbf{K}_L] + [\mathbf{K}_G]\right)\Delta\mathbf{u} = {}^{t+\Delta t}\overline{\mathbf{F}} - \mathbf{F} \tag{37}$$

where $\overline{\mathbf{F}}$ and $\mathbf{F}$ are the external and internal forces respectively.

The equilibrium equation must be satisfied throughout the complete history of loading and the non-linear processing will be stopped only when the out of balance forces are negligible within a certain convergence limit. If it is necessary to extend the stability analysis beyond the limit point, i.e. in the so-called post-buckling range, appropriate solution procedures must be applied. One approach is to use the arc-length control method in conjunction with the Newton- Raphson method to extend the stability analysis beyond the limit point, by Crisfield (1981).

7. Numerical Examples

Two numerical examples are solved to validate the performance of the shell element in geometrically nonlinear applications. The anisotropic composite materials are used for validation. Since the present study shows complex load-deflection curve, it is necessary to use the arc-length control method (Crisfield, 1981) in order to trace the full path of load-deflection. The automatic arc-length procedure (Chaisomphob *et al.*, 1988 and Ma *et al.* 1989) is used for tracing equilibrium paths of geometrically nonlinear shells.

The nonlinear analysis of laminated composite shell is carried out with a 3.175mm, 6.35mm and a 12.7mm thickness. The curved shell is hinged at the straight edges and free at the curved edges. The quarter model is used for cross ply laminated composite shells.

The material properties are young's modulus $E_1 = 3.3kN/mm^2$, $E_2 = E_3 = 1.1kN/mm^2$, shear modulus $G_{12} = G_{13} = 0.6kN/mm^2$, $G_{23} = 0.44kN/mm^2$, and Poisson's ratio $\nu_{12} = \nu_{13} = \nu_{23} = 0.25$. Lay up used is $90°/0°/90°$. The geometry of shell is shown in Fig. 5.

The Figure 6 shows the load-displacements curves for 12.7mm thickness. It is shown that the structure exhibits a limit point. Beyond the limit point, the response of the curved shell will be unstable with possibility of a snap-through behavior. The Figure 7 shows the load-displacements curves for 6.35mm thickness. The results shown in Figures 6 and 7, obtained with the present formulation are in complete agreement with those reported in the reference.

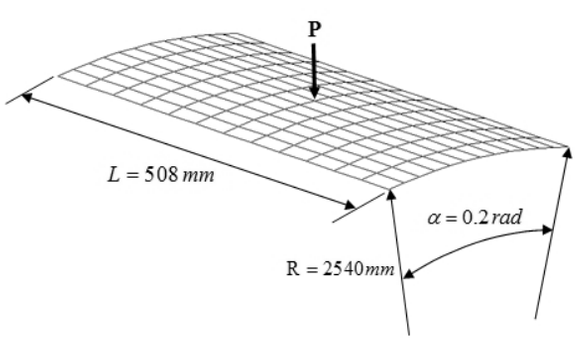

Fig. 5 Geometry of hinged shell

Next, we investigate the behavior of the hinged cylindrical shell for the thickness 3.175mm. The thickness is considered in the analysis that leads to a thin curved shell with ratio $R/h = 800$. Numerical results concerning the central deflection at the point load are shown in Figure 8. We see that the very thinner curved shell shows complex equilibrium paths with snap-through and snap-back behavior.

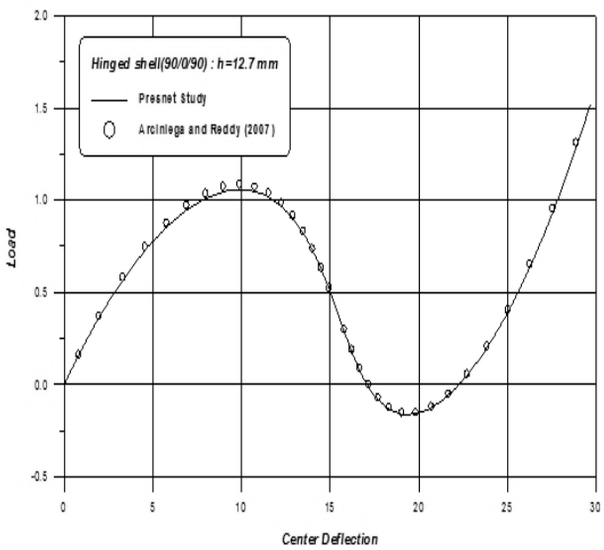

Fig. 6 Displacements of hinged cylindrical shell under point load (symmetric cross-ply (90/0/90), thickness=12.7mm)

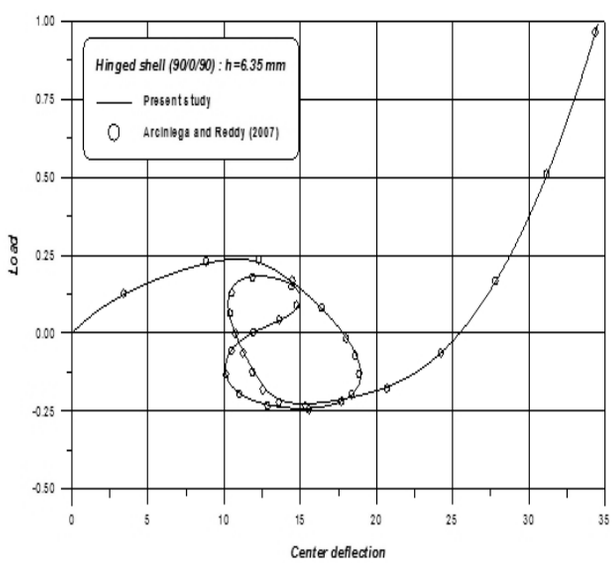

Fig. 7 Displacements of hinged cylindrical shell under point load (symmetric cross-ply (90/0/90), thickness=6.35mm)

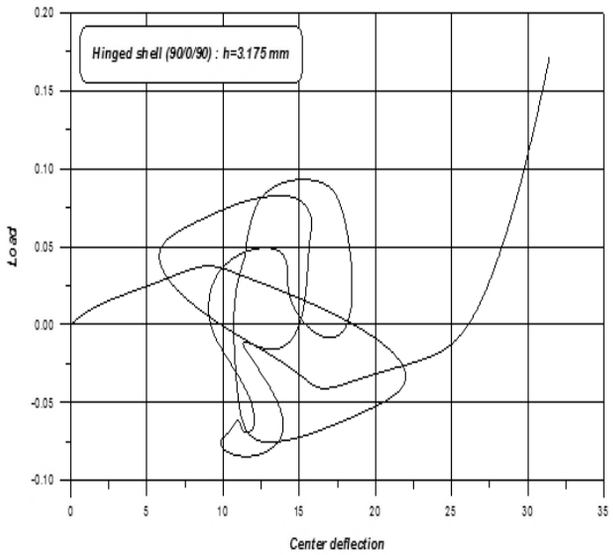

Fig. 8 Displacements of hinged cylindrical shell under point load (symmetric cross-ply (90/0/90), thickness=3.175mm)

8. Conclusions

In this paper we have developed an Element-Based Lagrangian Formulation for the nonlinear analysis of shell structures. In order to demonstrate the capability of the proposed shell element based on the Element-Based Lagrangian Formulation, non-linear problems are discussed above. The Element-Based Lagrangian Formulation makes implementation simpler and easier than the traditional Lagrangian formulations, especially when the assumed natural strain method is involved. Numerical examples for laminated composite curved shells presented herein clearly show the validity of the present approach and the accuracy of the developed shell element. Especially, a thin laminated composite shell may be the benchmark test for the large deformation analysis of a laminated composite shell element.

REFERENCES

Ahmad, S., Irons, B.M. and Zienkiewicz, O.C. (1970) Analysis of Thick and Thin Shell Structures by Curved Finite Elements. *Int. J. Num. Meth. Eng.*, 2, pp.419-451.

Arciniega, R. A. and Reddy, J. N. (2007) Tensor- based finite element formulation for geometrically nonlinear analysis of shell structures. *Comput. Meth. Appl. Mech. Eng.*, *196*, pp.1048-1073.

Crisfield, M.A. (1981) A fast incremental/iterative solution procedure that handles snap-through. *Comput. Struct.*, *13*, pp.55-62.

Han, S.C., Ham, H.D. and Kanok-Nukulchai, W. (2008) Geometrically non-linear analysis of arbitrary elastic supported plates and shells using an element-based Lagrangian shell element. *International Journal of Non-linear Mechanics, 43*, pp.53-64.

Han, S.C., Kim, K.D. and Kanok-Nukulchai, W. (2004) An element-based 9-node resultant shell element for large deformation analysis of laminated composite plates and shells. *Structural Engineering and Mechanics, 18*, pp.807-829.

Han, S.C., Lee, S.Y. and Rus, G. (2006) Postbuckling analysis of laminated composite plates subjected to the combination of the in-plane shear, compression and lateral loading. *International Journal of Solids and Structures, 43*(18-19), pp.5713-5735.

Han, S.C., Tabiei, A. and Park, W.T. (2008) Geometrically nonlinear analysis of laminated composite thin shells using a modified first-order shear deformable element-based Lagrangian shell element. *Composite Structures*, *82*, pp.465-474.

Han, S.C., Kanok-Nukulchai, W. and Lee, W. H. (2011) A refined finite element for first-order plate and shell analysis. *Structural Engineering and Mechanics, 40*, pp.191-213.

Hughes, T.J.R., and Liu, W.K. (1981) Nonlinear finite element analysis of shells: Part I. Three-dimensional shells. *Comput. Meth. Appl. Mech. Eng*., *26*, pp.331-362.

Kanok-Nukulchai, W. and Wong, W.K. (1988) Element-based Lagrangian formulation for large-deformation analysis. *Comput. Struct*., *30*, pp.967-974.

Kim K.D., Lomboy G.R. and Han S.C. (2003) A co-rotational 8-node assumed strain shell element for postbuckling analysis of laminated composite plates and shells. *Computational Mechanics*, *30*(4), pp.330-342.

Lee, S.J. and Kanok-Nukulchai, W. (1998) A Nine-Node Assumed Strain Finite Element for Large Deformation Analysis of Laminated Shells. *Int. J. Num. Meth. Eng. 42*, pp.777-798.

Liu, W.K., Lam, D., Law, S.E. and Belytschko, T. (1986) Resultant stress degenerated shell element. *Comput. Meth. Appl. Mech. Eng*., *55*, pp.259-300.

Park, W.T., Chang, S.Y. and Chun K.S. (2010) Comparison of Various Shear Deformation Functions for Laminated Composite/Sandwich Plates. *J. Korean Soc. Adv. Comp. Struc*., *3*(1), pp.1-9.